ACS OMEGA

http://pubs.acs.org/journal/acsodf

Article

Phytolith-Occluded Carbon Sequestration Potential of Oil Palm Plantation in Tamil Nadu

Veeraswamy Davamani,* Ramasamy Sangeetha Piriya, Srirangarayan Subramanian Rakesh, Ettiyagounder Parameswari, Selvaraj Paul Sebastian, Periasamy Kalaiselvi, Muthunalliappan Maheswari, and Rangasamy Santhi

Cite This: *ACS Omega* 2022, 7, 2809−2820

Read Online

ACCESS | Metrics & More | Article Recommendations

ABSTRACT: Oil palm (*Elaeis guineensis*) has proven to be a phytolith-occluded carbon (PhytOC)-rich species that plays a vital role in acting as a carbon sink for reducing atmospheric carbon dioxide (CO_2) concentration. The present research estimated the silicon, phytolith, and PhytOC contents in four (OP4), eight (OP8), and fifteen (OP15)-year-old oil palm plantations. Qualitative analysis using a scanning electron microscope (SEM) revealed the presence of abundant globular echinate phytoliths with varied diameter (8.484−10.18 μm) in fronds, empty fruit bunches, and roots. Furthermore, a wide band (400−490 cm^{-1}) underlined a higher relative abundance of Si−OH groups in empty fruit bunches, fronds, and roots, which emphasized the amorphous nature of silica. Quantitative analysis revealed that the phytolith (phytolith/dry biomass), PhytOC (PhytOC/phytolith), and PhytOC (PhytOC/dry biomass) contents in all oil palms differed significantly ($p < 0.05$) and increased with age. The PhytOC stock showed significant variation, with the trend of OP15 > OP8 > OP4. The belowground biomass of OP4 (16.43 g kg^{-1}) and OP8 (17.13 g kg^{-1}) had a maximum PhytOC concentration compared to the aboveground biomass, and the belowground proportion varied from 20.62 to 20.65%. The study demonstrated a positive correlation between the phytolith and PhytOC contents of oil palm; thereby, oil palm should be cultivated for enhanced long-term sequestration as a phytolith accumulator.

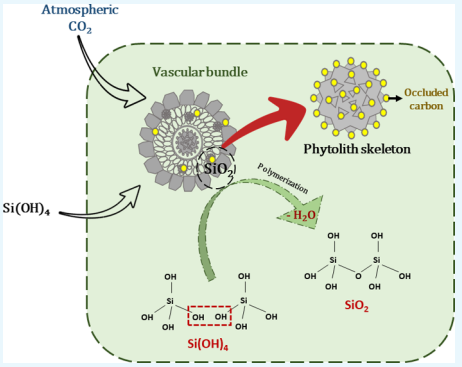

INTRODUCTION

The increasing atmospheric concentration of greenhouse gases is the leading cause of climate change and a major threat to the sustainability of the terrestrial ecosystem. A significant rise in the concentration of carbon dioxide (CO_2) of up to 31.5 Gt has occurred globally.[1] The increase in atmospheric temperature directly influences the soil respiration, thereby accelerating the release of a large amount of carbon from soil.[2,3] Therefore, climate change mitigation strategies are needed either to cut the emissions from the sources or to reduce the atmospheric CO_2 concentration through carbon sinks. Although soil stores carbon in large quantities, due to modified land use, complicated carbon storage processes, and continuously changing environmental circumstances, most organic carbon in soil cannot persist for an extended period.[4] Hence, finding a safe and effective long-term carbon sequestration mechanism is essential. Terrestrial biogeochemical carbon (C) sequestration is getting wider attention as the most promising approach for long-term storage.[5] Biotic C sequestration through occlusion of C within phytoliths is one of the practical approaches to climate change mitigation. Recently, phytolith-occluded carbon (PhytOC) demonstrated a significant role in long-term capture and storage of carbon.[2] The phytolith carbon sequestration potential via bamboo and/or other PhytOC-yielding agricultural crops was assessed to be ∼1.5 billion $tCO_2eq\ yr^{-1}$[6] globally.

Phytoliths are complex silicon-coated carbon substances that are also called amorphous silica (Si), formed in cells through biosilicification. During biosilicification, Si is absorbed by the root system in the form of soluble silicic acid [$Si(OH)_4$] and carried to different plant parts through the vascular system. The Si gets precipitated at neutral pH and deposits in the leaves, stem, roots, inflorescence, etc.[7] Although Si is not considered a crucial element for plant growth, it has multiple beneficial effects, which include development, yield, mineral nutrition, health, and survival of plant species for decades in agricultural ecosystems. It provides rigidity, enhances resistance to plant abiotic−biotic stresses, and influences element cycling during litter decomposition.[8] The accumulation of

Received: October 7, 2021
Accepted: December 24, 2021
Published: January 10, 2022

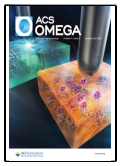

https://doi.org/10.1021/acsomega.1c05592
ACS Omega 2022, 7, 2809−2820

Table 1. Site Characteristics of Sampling Plots of Oil Palm Plantation

location	age group	abbreviation	latitude (°E)	longitude (°N)	area (ha)	density (plants ha^{-1})
Muthalakampatti	4	OP4	10.03	77.61	10.0	1520
Bommaiyagoundenpatti	8	OP8	10.04	77.47	3.30	450
Upparpatti	15	OP15	9.93	77.41	2.05	270

intercellular and extracellular phytoliths in the plant parts is aided by the system's evaporation and water transportation. Generally, phytoliths are highly stable and possess distinctive shapes with varied dimensions (20−200 μm).[9] They can survive in harsh environmental conditions due to their outer silicon layer that is resistant to weathering, and are preserved in the soil or sediments for millions of years after plant decomposition. Phytolith-occluded carbon (PhytOC) is the stable organic C fraction entrapped within the phytolith, accounting for 0.1−5.8%.[10−14] They are also used in paleoecological, archaeological, and paleoenvironmental reconstructions to study vegetation dynamics.[15] Arecaceae (palms) family species are prolific phytolith producers,[15] and the Si concentration in the plants ranges from 0.1 to 16% dry weight.[16,17] The Si deposition takes place on the plant cell wall in cortex intercellular spaces and cell lumen infilling, essential to living cell morphology. It is abundant in commelinid monocots, especially Poaceae, Cyperaceae, Bambusoideae, Zingiberales, and Arecaceae.[18,19] The phytolith composition varies with different species growing in the same environment and soil. The chemistry and the elemental composition of phytoliths is heavily influenced by environmental factors like plant taxa, soil composition, climatic conditions, pH, temperature, and the location within the tissue[20] and geochemical conditions.[21] The concentration of phytoliths in wetland Poaceae and Cyperaceae species is 10−15%, but it can reach 0.5% or less in dicotyledons and 1−3% in typical grasses of dryland.[22] Studies have evaluated the phytolith content and PhytOC concentration in bamboo species,[6] native grasses,[23] millet,[24] peat-land soil,[25] sugarcane cultivars,[26] and wheat.[27]

Specifically, PhytOC shows significant potential in long-term C sequestration by accounting for up to 82% of the total carbon in well-drained soils after 2000 years of organic matter decomposition.[28] The PhytOC concentrations in different plants vary greatly due to their differences in the capacity for Phytolith accumulation.[28] But it is difficult to estimate the total amount of phytolith because of its massive distribution in plant parts. Recent advancements have shown the ability to identify palm phytoliths in the mid-elevation Andean forest,[15] monopodial bamboo in China,[28] Amazonian forests,[29] and Brazilian shrub.[30] Understanding of PhytOC in oil palm plantations as region-specific and its potential in long-term C sequestration will be an added advantage. To the best of our knowledge, there are no reports on phytolith estimation in the oil palm plantations of India and hence, we attempt to survey the oil palm plantations in Tamil Nadu for phytolith research. In line with the context, this study was focused to characterize and compare the phytolith morphology variations in three different-aged oil palms (4, 8, and 15 years), and estimated the carbon stocks concerning the belowground and aboveground biomass of different-aged oil palm plantations. We hypothesize that the PhytOC make a significant contribution to the total C sequestration of oil palm. This would enhance the knowledge regarding the variations in Si content and help to understand the scope and potential of oil palm in C sequestration in the agricultural ecosystem. Moreover, it will provide a scientific foundation for research on PhytOC sink in the oil palm plantation (Table 1).

RESULTS AND DISCUSSION

Soil Physicochemical Properties. The soil properties were varied for OP4, OP8, and OP15, and significant differences ($p < 0.05$) were observed in pH, EC, bulk density, and soil organic carbon (Table 2). Soil bulk density was higher for OP8 (288 Mg m^{-3}) than for OP4 (117 Mg m^{-3}) and OP15 (175 Mg m^{-3}). Further, the soil organic carbon increased (0.51−0.68%) when soil pH was decreased (7.15−6.81) from OP4 to OP8. The observations followed the study of estimating the soil properties (pH and bulk density) at three steppes with significant difference.[31] The soil with low pH is reported to take up Si and accumulate more, thereby showing a higher PhytOC content.[28]

Table 2. Soil Characteristics of the Oil Palm Plantations[a]

soil parameters	OP4	OP8	OP15
pH	7.15b	6.81b	7.54b
EC (dS m^{-1})	0.29c	0.40c	0.25b
bulk density (Mg m^{-3})	117a	288a	175a
Soil Carbon Fractions			
organic carbon (%)	0.51b	0.68b	0.71b
total carbon (%)	0.73b	0.84b	0.85b
microbial biomass carbon (μg g^{-1} of soil)	5.37a	6.6a	7.08a

[a]Note: Means with different lowercase letters in a column indicate a significant difference at $P = 0.05$ based on the least significant difference (LSD) test.

When oil palm fronds, fibers, sheath, EFB, etc. are returned to the soil, phytoliths are released into the soil after *in situ* decomposition, and this would aid in the occlusion of CO_2 into phytoliths. Therefore, soil organic carbon status (0.51−0.71%) is improved from OP4 to OP15, and PhytOC could be considered as an important part of the soil stable organic C.[32]

Belowground and aboveground biomass of OP4, OP8, and OP15 plantations. The aboveground biomasses (AGB) of OP4, OP8, and OP15, including fronds, sheath fiber, and empty fruit bunches, were 74.90, 97.90 and 158.80 t ha^{-1} (Table 3). The belowground biomass (BGB), including roots, was smaller than the aboveground biomass, ranging between 19.50 and 41.30 t ha^{-1} for OP4, OP8, and OP15. Although BGB was lower than AGB, both the contents were increased from OP4 to OP15. The BGB proportion of OP4, OP8, and OP15 varied from 20.62 to 20.65%. Furthermore, it was analyzed in the three steppes (dessert steppe, wet typical

Table 3. Biomass of the Oil Palm Plantations

oil palm plantation	AGB (t ha^{-1})	BGB (t ha^{-1})	total biomass (t ha^{-1})	ratio of BGB to total biomass (%)
OP4	74.90	19.50	94.4	20.65
OP8	97.90	25.45	123.35	20.63
OP15	158.90	41.30	200.2	20.62

https://doi.org/10.1021/acsomega.1c05592
ACS Omega 2022, 7, 2809−2820

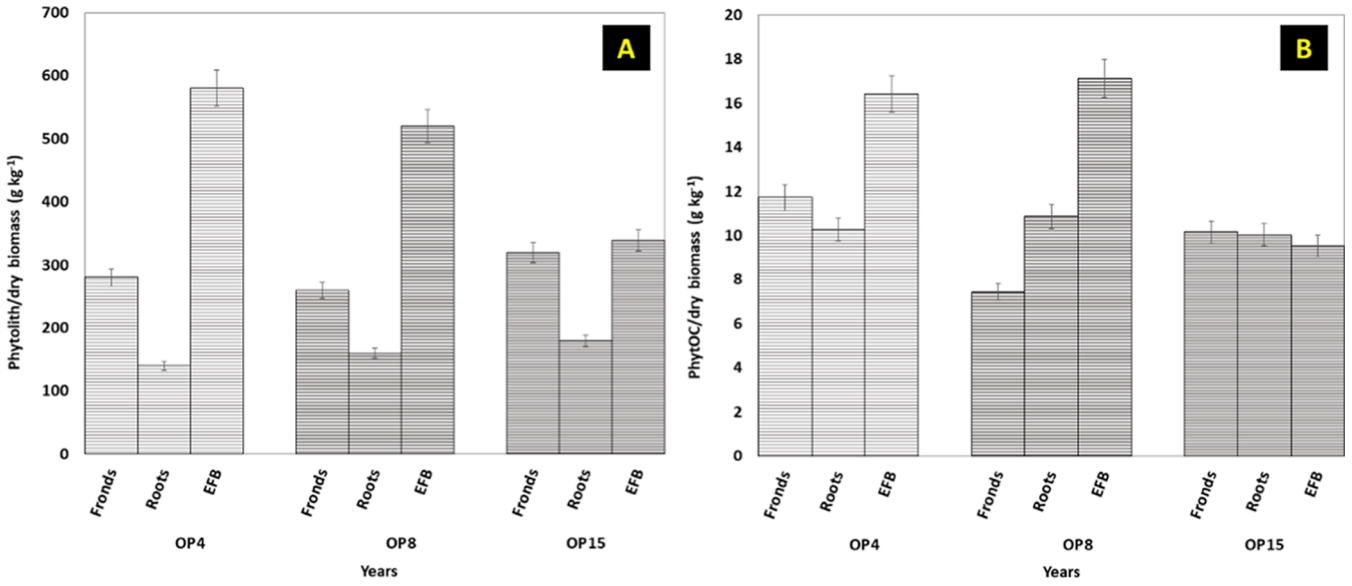

Figure 1. Comparison of phytolith/dry biomass (A) and PhytOC/dry biomass (B) in different-year-old oil palm plantations.

Table 4. PhytOC Stock in Parts of Oil Palm

age group (yr)	aboveground PhytOC stock (kg ha^{-1})	belowground PhytOC stock (kg ha^{-1})	plant PhytOC stock (kg ha^{-1})	total area (ha)	total belowground PhytOC stock (t)
4	732.69	190.75	923.45	10.0	9.23
8	1406.25	365.57	1771.82	3.30	5.85
15	1651.76	429.31	2081.08	2.05	4.27

steppe, and dry typical steppe). The estimated AGB and BGB were higher compared to the dessert steppe (562.27 and 4227.9 kg ha^{-1}), wet typical steppe (1471.99 and 8639.89 kg ha^{-1}), and dry typical steppe (1120.09 and 8643.74 kg ha^{-1}).[31] Furthermore, they were higher than the monopodial bamboo's AGB (20.82 to 48.68 t ha^{-1}) and BGB (5.78 to 62.16 t ha^{-1}).[28]

Phytolith Content and Concentration of PhytOC in Belowground and Aboveground Biomass of OP4, OP8, and OP15 Plantations. The phytolith content, C concentration in phytolith (PhytOC in phytolith), and PhytOC content were compared (Figure 1) between the three stages of plantations. The amount of Si varied from 0.1 for fronds to 4.3 g kg^{-1} for roots in all age groups of oil palm. No significant variation was found in the Si content of OP4, OP8, and OP15. Besides, the phytolith content ranged from 140 to 580 g kg^{-1}, with maximum in the roots of OP4 (580 g kg^{-1}), followed by OP8 (520 g kg^{-1}) and OP15 (340 g kg^{-1}). The concentration of carbon in phytolith ranged between 28.03 and 67.92 g kg^{-1}, with a higher concentration in the phytolith of the EFB of OP4 (73.41 g kg^{-1}), OP8 (67.92 g kg^{-1}), and OP15 (55.78 g kg^{-1}). The C concentrations in the phytolith of OP4, OP8, and OP15 were higher than that of the rice,[33] Lei bamboo litter,[34] foxtail millet,[35] and herb species[36] of the forests (Betula, Quercus, Larix, and Pinus), whereas they were lower than those of sugarcane[26] and wheat.[27]

Further, the concentration of PhytOC in dry biomass varied between 7.44 and 17.13 g kg^{-1}, wherein the maximum PhytOC was estimated in the roots of OP4 (16.43 g kg^{-1}) and OP8 (17.13 g kg^{-1}), while minimum in the case of OP15 (9.53 g kg^{-1}). The phytolith and PhytOC content in the oil palm plantations follow the order OP4 < OP8 < OP15. The difference in phytolith and PhytOC content in plant species varied in physiological properties and their adaptation to environmental conditions. Being a monocot, oil palm accumulates more Si than non-monocots.[31] Not only the phylogeny, but also the soil (water and pH) and efficiency of C encapsulation by the Si will influence the plant Si uptake, accumulation of soil phytolith, and bioavailability of Si.[28] The estimated amounts of phytolith and PhytOC in OP4, OP8, and OP15 were higher than the concentrations present in eight monopodial bamboo species (37−122 and 4.3 g kg^{-1}).[3] Furthermore, the results of this study were higher than the estimated phytolith and PhytOC content in the rhizome (11.20−34.93 and 0.34−0.83 g kg^{-1}) and belowground trunk (5.88−14.95 and 0.1−0.94 g kg^{-1}) of monopodial bamboo[28] and steppes in northern China.[31] In addition to that, a statistical analysis was also performed to determine the relationship of phytolith/dry biomass with PhytOC/phytolith and PhytOC/dry biomass in OP4, OP8, and OP15. It was found that there was a significant linear correlation of phytolith/dry biomass with PhytOC/phytolith (R^2 = 0.5522) and PhytOC/dry biomass (R^2 = 0.6279) (Figure 3). Similarly, the phytolith and PhytOC contents of Chinese grassland have a positive linear correlation.[37] The significant correlation in the vegetation among different forests indicated that increasing phytolith production could promote the phytolith C sequestration potential.[36] It is been suggested that appropriate management practices could increase the PhytOC flux and thereby phytolith carbon sink. It is reported that through scientific management practices the silica content could be improved, including silica fertilization,[38] irrigation, and genetic engineering,[39] which would augment the total biomass production, boosting Si uptake and ultimately phytolith C sequestration.[40] For instance, global cropland has tripled phytolith C sequestration since 1961 due to the cropland expansion, fertilization, and irrigation.[41]

https://doi.org/10.1021/acsomega.1c05592
ACS Omega 2022, 7, 2809−2820

PhytOC Stock in Belowground and Aboveground Biomass of OP4, OP8, and OP15 Plantation. The available PhytOC stock in the AGB of OP4, OP8, and OP15 was 732.69, 1406.25, and 1651.76 kg ha^{-1}, respectively. An increase in the PhytOC content was observed moving from OP4 to OP15 (Table 4) and compared under different biomasses (Figure 2). The AGB proportion of OP4, OP8, and OP15 from the total PhytOC stock varied between 79.34 to 79.37%. In addition, the BGB was maximum for OP15 (429.31 kg ha^{-1}) compared to OP4 (190.75 kg ha^{-1}) and OP8 (365.57 kg ha^{-1}). According to the distribution area of OP4 (10 ha), OP8 (3.30 ha), and OP15 (2.05 ha), the total belowground PhytOC stock was estimated as 9.23, 5.85, and 4.27 t, respectively. The available PhytOC stock of OP4, OP8, and OP15 was higher than that in millet (5.45 kg ha^{-1}),[42] grassland (1.64−10.36 kg ha^{-1}),[37] wheat (1.64−10.36 kg ha^{-1}),[27] rice (7.09−34.09 kg ha^{-1}),[33] wetland (0.82−21 kg ha^{-1}),[43] sugarcane (32.73−98.18 kg ha^{-1}),[26] monopodial bamboo,[28] major steppes,[31] and Lei bamboo stand (AGB 13.0 and BGB 12.8 kg ha^{-1}).[44]

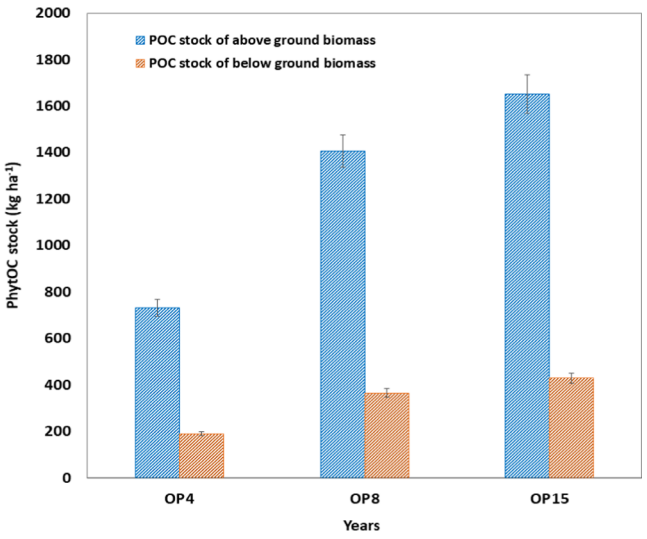

Figure 2. Comparison of PhytOC stock in different-year-old oil palm plantations.

The results suggested that though the AGB is higher than the BGB of OP4, OP8, and OP15, the PhytOC concentrations in the BGB of OP4 (16.43 g kg^{-1}) and OP8 (17.13 g kg^{-1}) are relatively higher than AGB concentrations. This is due to the perenniality of the oil palm plants.[31] Thus, the BGB could significantly contribute to the PhytOC stock in the belowground, which could be explained by the higher phytolith accumulation capacity in the oil palm and higher biomass. In contrast, the PhytOC stock in BGB was remarkably lower than the AGB of OP4, OP8, and OP15. The focus should be given to the BGB phytolith and its PhytOC content, which is similar to the findings on the PhytOC concentration of bamboo plants.[28] The findings of this study substantiate the hypothesis and suggest that oil palm is a potential phytolith accumulator with higher PhytOC concentration in BGB and AGB (Figure 3).

Surface Analysis of Si in Oil Palm Plantation. A detailed investigation of the dispersed phytolith represented different morphologies, wherein ellipsoid phytoliths were observed in the EFB (Figure 4a). Several silica craters are uniformly observed over the surface with perforated bottoms indicating that silica accretion on EFB is an ensuing biological process rather than a random event. Such a genetic design emphasizes the biological necessity for oil palm trees providing multifunctional abilities in addition to nutritional needs.[45] The surface orientation of the phytolith showed an acute profile, possessing multiple peaks and a medium phytolith density of 15−30, which is similar to the *Metroxylon vitiense* inflorescence.[46] In addition, Si phytolith as a globular echinate with fusiform edges is identical to *Acrocomia aculeata*.[47] The average diameter of the phytolith in EFB was 8.484−10.18 μm, which was analogous to *Borassus aethiopum*, *P. canariensis*, *T. fortune*, *C. alba*, and *Texania campestris*.[48] The diameter was threefold higher than *Billbergia sp.*,[47] 25% higher than *Metroxylon sagu*, and 10% higher than *Cocos nucifera*.[49] The phytolith in the fronds is in association with sclerenchyma and epidermal cells.[50]

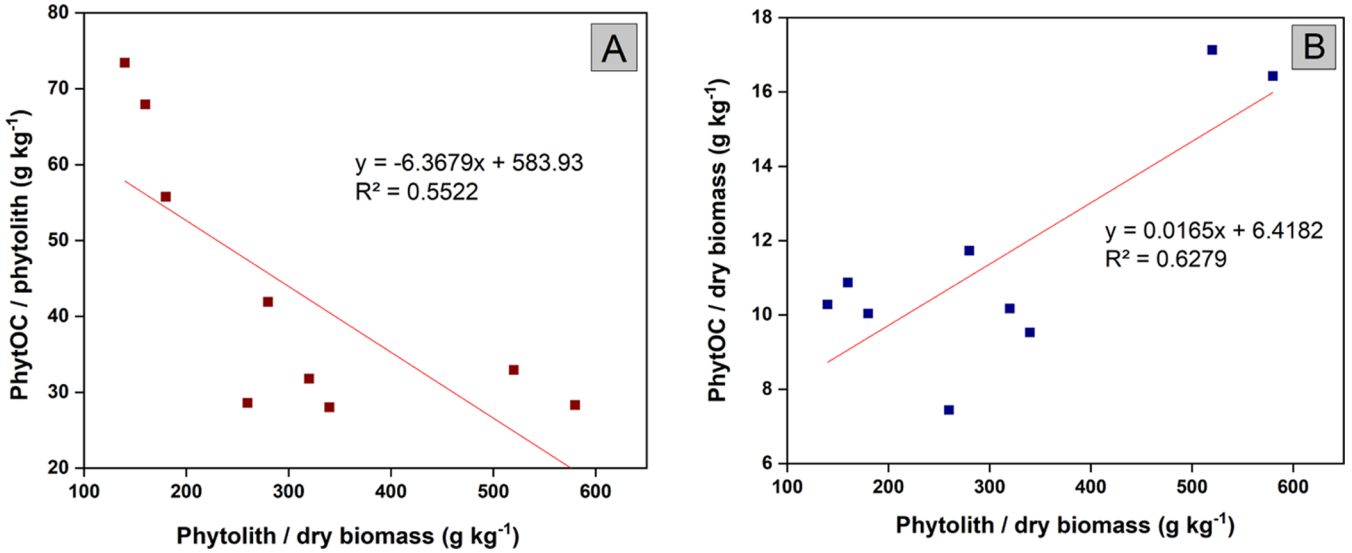

Figure 3. Correlation between parameters (A) phytolith/dry biomass and PhytOC/phytolith and (B) phytolith/dry biomass and PhytOC/dry biomass.

https://doi.org/10.1021/acsomega.1c05592
ACS Omega 2022, 7, 2809−2820

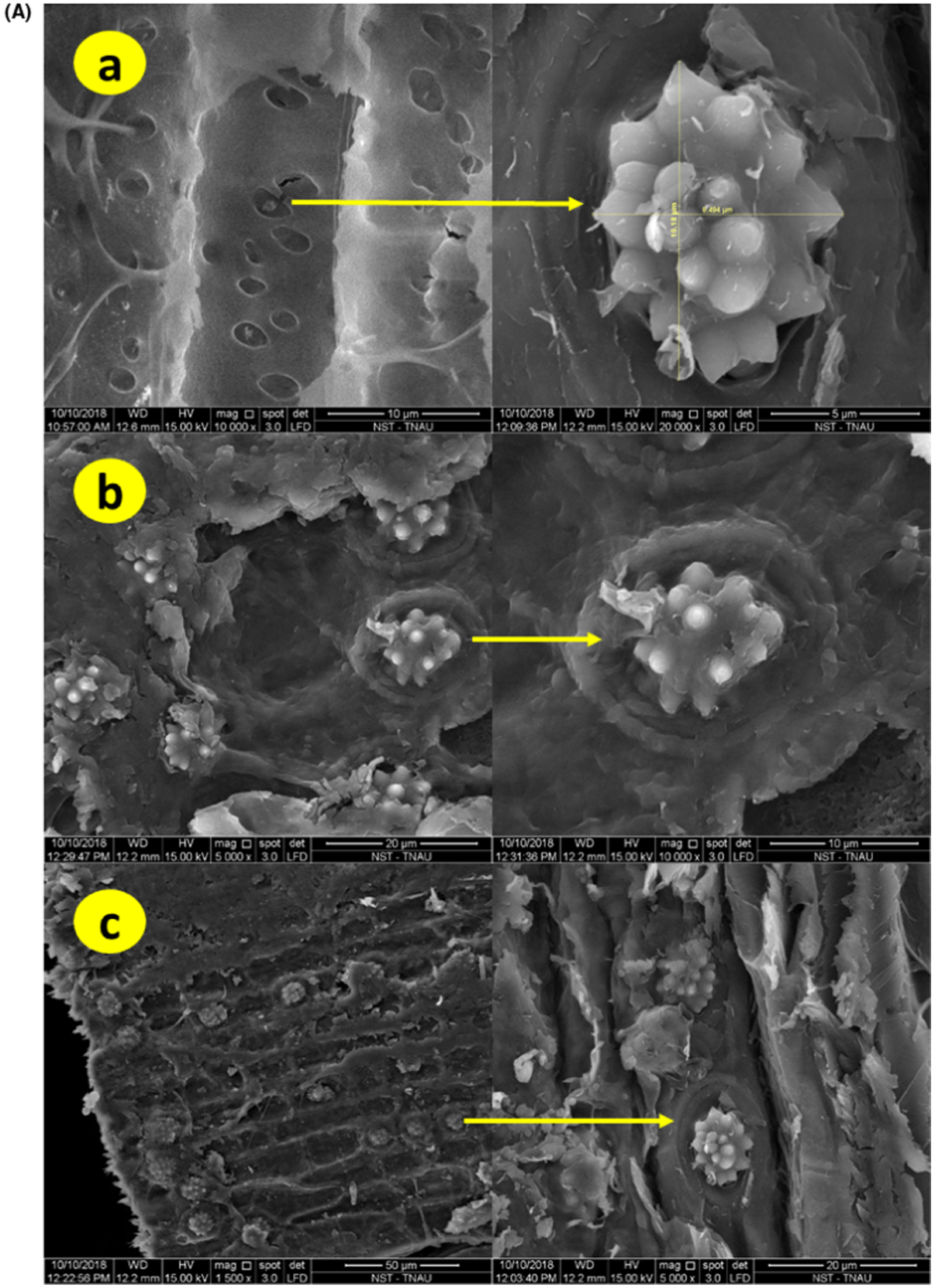

Figure 4. continued

https://doi.org/10.1021/acsomega.1c05592
ACS Omega 2022, 7, 2809−2820

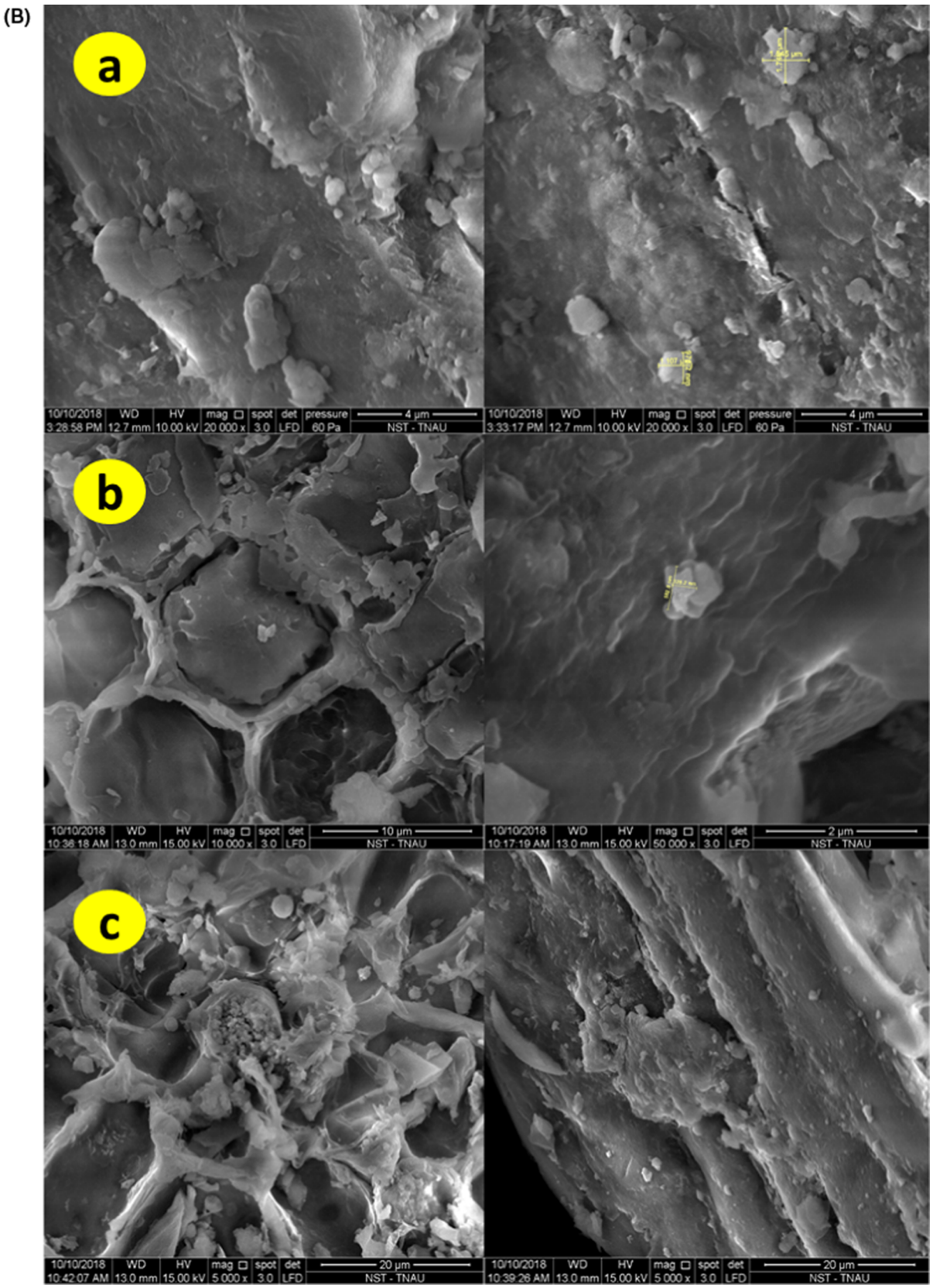

Figure 4. continued

https://doi.org/10.1021/acsomega.1c05592
ACS Omega 2022, 7, 2809−2820

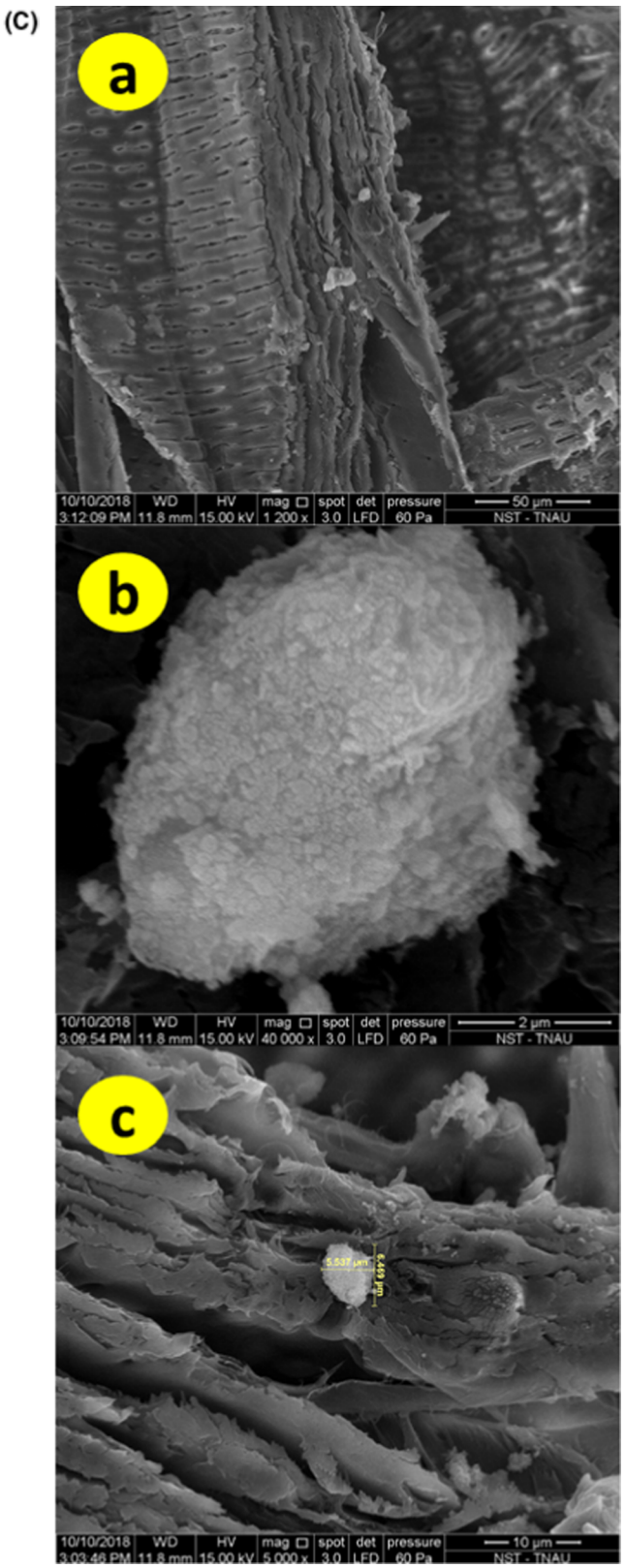

Figure 4. (a) SEM micrographs of phytoliths in empty fruit bunches of (a) OP4, (b) OP8, and (c) OP15. (b) SEM micrographs of phytoliths in fronds of (a) OP4, (b) OP8, and (c) OP15. (c) SEM micrographs of phytoliths in roots of (a) OP4, (b) OP8, and (c) OP15.

The oil palm fronds have an abundant globular echinate phytolith (Figure 4b) created in parenchyma tissues. The observations were comparable to palm leaf phytoliths of *Trachycarpus fortune* and *Phoneix canariensis*, *Zingiber officinales*, *Hyphaene* spp., *Billbergia* sp, *P. notatum*, *Bromus auleticus*, *A. compressus*, *M. sagu*, *A. catechu*, *B. aethiopum*, *Calamus aruensis*, and *Pitcairnia feliciana*.[48,49,51−54] Besides, there was

https://doi.org/10.1021/acsomega.1c05592
ACS Omega 2022, 7, 2809−2820

also a rectangular phytolith of 328−582 nm diameter, similar to *Hydriastele boumae* leaf.[46]

The Si phytolith in the roots (Figure 4c) is present at an irregular distance, with an average size between 5.437 and 6.459 μm. The compaction and the distance between the phytoliths were between 5 and 8 μm. Moreover, phytoliths were asymmetric in morphology with columellate profiles. The phytolith density was more than 30, similar to the *Juania australis* leaf.[46] The spines tapering at the top of the phytoliths were conical and varied between 12 and 21 spines. The results were in parallel to the spines of *C. aruensis*, *C. nucifera*, *Butia capitata*, *Phoenix canariensis*, *T. fortune*, and *Trithrinax campestris*. The average spine length (2.68 μm) was two-fold higher than that of *T. fortune* and *B. capitata* and four-fold higher than that of *C. aruensis*.[47,48]

The EDX analysis reported a higher amount of three elements (Si, C, and O) in the Si phytoliths of the EFB, fronds, and roots (Figure 5). The higher amount of C was attributed to the surface coating of the sample upon analysis under SEM. The phytolith in the tissues of date palm, *Phenix dactilyfera*, showed a dominance of Si and O.[55]

Surface Functionalities (FTIR Spectrum). The spectroscopic study showed peaks in the FTIR spectrum (Figure 6). The broadband at 3428.81 cm^{-1} corresponds to the O−H stretching of hydrogen-bonded hydroxyl groups of cellulose and absorbed water. The OH peak exhibited the hydrophobic properties present in the natural fibers of the fronds.[56−58] The peaks at 1639.2 and 1074 cm^{-1}were fingerprint regions corresponding to the different vibrations of the cellulose and hemicellulose groups.[59] The band at 2925.48 cm^{-1} was attributed to the C−H aliphatic group stretching that marked methylene groups' existence in cellulose and the symmetric vibration of CH_2 groups.[58] The ester of the group C═C aromatic group was found at 611.32 and 1639.2 cm^{-1} corresponding to the C═O stretching of the amide group.[60] The peak at 1428.99 cm^{-1} represents the CH_2 bending present in the aromatic lignin groups. The peak at 1265.07 cm^{-1} (C−O−C) indicates the ether band between the hydroxyl group's lignin and carbohydrates. The peak at 1074.16 cm^{-1} indicates the stretching of C−O−C.[61] FT-IR studies of EFB, fronds, and roots of oil palm showed similarities to the spectrum of palm oil.[62] Similar bands were observed in oil palm biomass, representing the O−H stretching at 3384−3421 cm^{-1} of cellulose and lignin. The peak at 2919 cm^{-1} represented the C═O stretching of the COOH group in hemicelluloses.[63]

Besides, the appearance of the wide band emphasized the amorphous nature of the silica in the 400−490 cm^{-1} range, ascribed to the Si−O−Si bond-rocking vibration in all three spectra (EFB, fronds, and roots). The large and asymmetrical band around 779 cm^{-1} visible in the root spectrum was ascribed to the Si−O−Si stretching from the heterogenic geometry of SiO_2 units, which is not observed in the fronds and EFB spectra. The enormous Si−OH groups and the existence of chemical impurities were reflected by the Si−O vibrations of non-bridging oxygen throughout the zone (950−1000 cm^{-1}) of the EFB spectra. Meanwhile, the spectrum of the fronds and root depicted lower Si−OH groups, representing the compact structure of phytolith present in the fronds and roots. The Brunauer−Emmet−Teller (BET) surface area analysis of the fronds (257.61 m^2 g^{-1}), roots (271.86 m^2 g^{-1}), and EFB (359.99 m^2 g^{-1}) were also in line with the observations of the FTIR spectrum. The higher

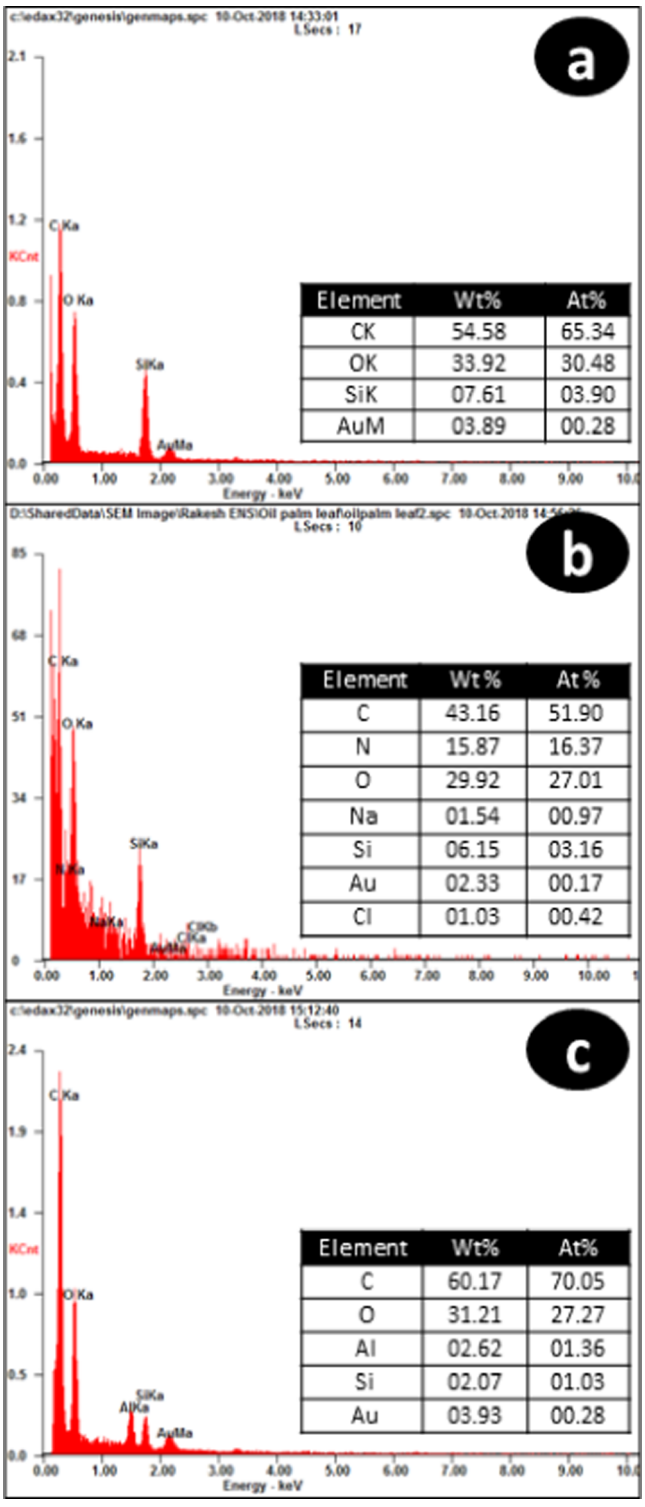

Figure 5. EDX of phytolith in oil palm: (a) empty fruit bunches, (b) fronds, and (c) roots.

relative abundance of Si−OH groups indicated a higher surface area of phytoliths in EFB compared to fronds and roots.[55]

PhytOC Long-Term Sequestration Potential. There is an opportunity to enhance the long-term and short-term carbon sequestration by growing high-PhytOC-yielding plant species primarily from Poaceae and Cyperaceae families. Some prolific producers of PhytOC are maize, rice, wheat, sorghum, sugarcane, wheat, and barley. Thus, the environmental

https://doi.org/10.1021/acsomega.1c05592
ACS Omega 2022, 7, 2809−2820

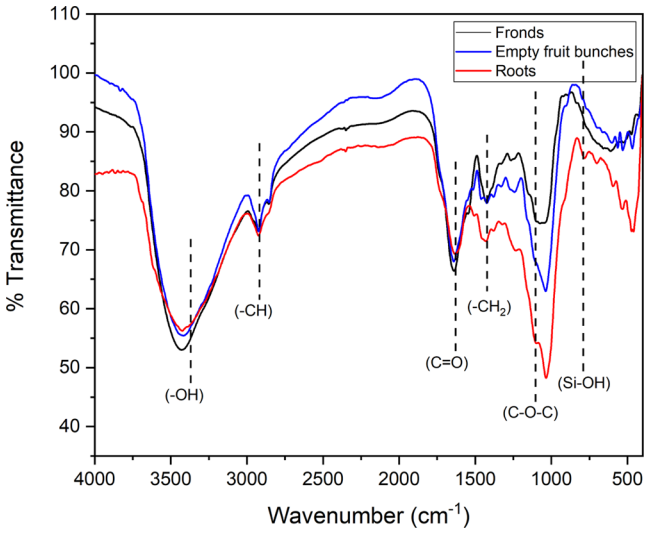

Figure 6. Surface functionalities of phytolith in oil palm: (a) empty fruit bunches, (b) fronds, and (c) roots.

conditions can be optimized for higher PhytOC production in plants, and this opportunity can be maximized by controlling other related factors. Studies have shown that it is relatively accurate to measure the whole biomass like AGB and BGB to understand the PhytOC stockpile and PhytOC concentration in the plant species. Therefore, this study demonstrates the measurement of available PhytOC in both AGB and BGB of oil palm plantations. Specifically, the BGB assessment showed a maximum production rate and stock in OP4 (20.65%), OP8 (20.63%), and OP15 (20.62%), indicating the importance of studying it in much depth. As shown in this study for oil palm roots, fronds, and EFB, there is a strong positive correlation between phytolith production and PhytOC content (Figure 3). This is the first field study that examined the change in PhytOC storage using a chronosequence method. To the best of our knowledge, this is the first field evidence in India that increasing PhytOC storage with long-term stability can be achieved through management approaches, stressing the need to investigate soil PhytOC storage under the effect of diverse soil physical and chemical features. By adding litters, the accumulation of PhytOC in oil palm plantation soils may be further increased, and it is considered to be another effective way of increasing soil PhytOC storage. Thus, it will effectively increase the long-term storage of organic C in intensively managed systems, with significant implications in mitigating climate change and enhancing the ecological services of such ecosystems. This study also describes the relation of the PhytOC production with the age of the oil palm, which is directly proportional. It is consistent with the previous findings on the BGB and AGB of monopodial bamboo[3] and major steppes[31] in China. Hence, the study of PhytOC in oil palm plantation necessitates further investigations on the factors influencing long-term sequestration, focusing on BGB (Figure 7).

CONCLUSIONS

The current study reveals that the phytolith-occluded carbon (PhytOC) concentration varied in different age groups such as OP4, OP8, and OP15, with their BGB (roots) showing the maximum concentration among other portions. A focused investigation is needed to quantify the PhytOC production flux and PhytOC sequestration capacity of oil palm from belowground biomass compared to the aboveground biomass. Both the phytolith content and PhytOC content in the oil palm are increased with increasing age (OP4 < OP8 < OP15). The accumulated PhytOC further boosts up the biomass content of the oil palm. Based on our results, nearly 162.7 (OP4), 237.8 (OP8), and 400.6 t (OP15) of CO_2 sequestration could be possible by the oil palm plantation in a hectare. The positive correlation between phytolith and PhytOC content indicates that oil palm is a potential phytolith accumulator. The study demonstrates that the available PhytOC constitutes a considerable portion of the passive carbon pool. Its accumulation in the soil will improve PhytOC collection, production, and subsequently terrestrial carbon sequestration. Thus, phytolith accumulators such as oil palm should be cultivated for enhanced long-term sequestration.

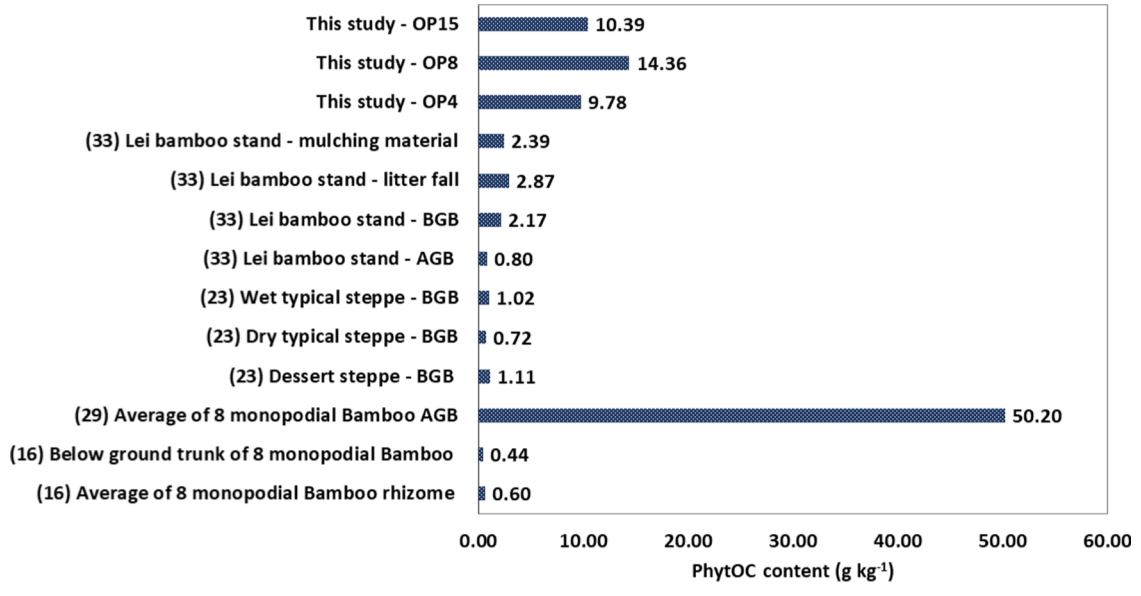

Figure 7. Comparison of the estimated PhytOC content in different biomasses by different authors.

https://doi.org/10.1021/acsomega.1c05592
ACS Omega 2022, 7, 2809−2820

METHODS

Study Area, Sample Collection, and Pretreatment. The selected plantations in the Theni district of Tamil Nadu had four-, eight-, and fifteen-year-old oil palm trees with a plant density of 1520, 450, and 270 per hectare. Three replicate plots were randomly selected for the collection of soil samples and parts of *Elaeis guineensis* (fronds, empty fruit bunches (EFB), and roots) from 4 (OP4), 8 (OP8), and 15 (OP15) year-old oil palm plantations. The sampling site details are tabulated in Table 1. Further, the soil samples were collected at a regular depth of 0−20, 20−40, and 40−60 cm from each random plot. The soil samples were dried and ground for physicochemical analysis (Table 2). The collected parts were thoroughly washed with deionized water and kept in the hot air oven (48 h @ 60 °C) for attaining constant weight.[8] The plant samples were dried at 70 °C for 48 h and ground (0.25 mm) for further analysis.

Phytolith and PhytOC Measurements. Soil pH and electrical conductivity (EC) were measured using a pH meter (M/s Elico, India) and an EC meter (M/s Elico, India). The Si estimation was performed using ICP-OES and the extraction of phytolith was carried out through microwave digestion.[8] The extract was dried in an oven at 65 °C for 48 h and weighed. A 0.8 M Potassium dichromate ($K_2Cr_2O_7$) solution was used to detect the organic content bound to the phytolith, and the alkali spectrophotometric method was used for estimating PhytOC.[28] In a typical procedure, a small amount of phytolith (0.01 g) was mixed with 10 M NaOH (0.5 mL) and kept at room temperature (25 °C) for 12 h for getting a proper solution. Further, the obtained solution was treated with 0.8 M $K_2Cr_2O_7$ (1.0 mL), concentrated H_2SO_4 (4.6 mL) was added to release the bound organic C, then kept in the water bath for 1 h at 98 °C, and PhytOC concentration was determined at 590 nm spectrophotometrically.[64]

The working standards (0, 20, 40, 60, 80, and 100 ppm) were prepared from the standard organic solution (1000 ppm 45 KHP) explained in the literature.[65] In the glass tube, 1 mL of $K_2Cr_2O_7$ (0.8 Mol L^{-1}) and 4.6 mL of H_2SO_4 were added and heated in a water bath (98 °C) for an hour. After cooling, 25 mL of distilled water was added, and the solution was transferred to 50 mL plastic tubes for centrifugation at 2500 rpm for 10 min. Finally, the solutions were taken to read at 590 nm in a UV−vis spectrophotometer.[66]

Phytolith Characterization and Calculations. The morphological features and size of the phytolith in the EFB, fronds, and roots of oil palm were investigated using a scanning electron microscope (SEM, M/s FEI—Quanta 250, Czech Republic) with an energy dispersive X-ray analyzer (EDX). Phytoliths of EFB, roots, and fronds were visualized under the SEM, wherein an electron beam strikes the surface and is backscattered with some energy signals carrying the information about the surface, which are amplified and translated into images. EFB, roots, and fronds biomass were dusted on the carbon stub kept under vacuum and mounted on the sample stage for the images at 8−10 KV and 3000−15 000× magnification.

Further, Fourier transform infrared spectroscopy (FT-IR) is used to study the surface functionalities of the EFB, fronds, and roots of oil palm under Model 8400 S of Shimadzu, Japan. The spectra were recorded for 0.5 mg of biomass entrenched with 0.1% potassium bromide (KBr) solution. A curve generated with wavenumbers 400−4000 cm^{-1} along the x-axis and percent transmittance along the y-axis indicates the peaks of functional groups vibrating at a specific frequency.

Brunauer−Emmet−Teller (BET) surface area analysis of the fronds, roots, and EFB was done using Quantochrome TouchWin, which involves adsorption of nitrogen gas molecules onto the surface of the biomass in the sample tube at −196 °C temperature in the presence of liquid nitrogen. The amount of gas adsorbed forming a monolayer is indicated as the specific surface area of the adsorbent carbon.[67]

The total dry mass of the aboveground organic material present in different oil palm parts, such as the fronds and empty fruit bunches, is known as the total aboveground biomass (AGB), while that of the biomass of roots is known as the total belowground biomass (BGB). The AGB and BGB were separately analyzed. The concentration of C in phytolith, PhytOC concentration, and PhytOC stock were estimated for fronds, roots, and EFB of different age-group oil palm trees through the following formulas[3]

$$\text{concentration of phytolith (g kg}^{-1}) = \frac{\text{weight of phytolith (g)}}{\text{dry biomass (kg)}} \quad (1)$$

$$\text{concentration of } C \text{ in phytolith (g kg}^{-1}) = \frac{\text{phytolith carbon (g)}}{\text{weight of phytolith (kg)}} \quad (2)$$

$$\text{PhytOC concentration (g kg}^{-1}) = \frac{\text{Phytolith carbon (g)}}{\text{Dry biomass (kg)}} \quad (3)$$

$$\text{PhytOC stock (kg ha}^{-1}) = \Sigma\{\text{POC concentration (g kg}^{-1}) \times \text{biomass (kg ha}^{-1}) \times 10^{-3}\} \quad (4)$$

Besides, the statistical analysis and data processing were performed using MS Excel and SPSS 18 software. The difference in phytolith and PhytOC concentration in the oil palm parts was examined through one-way ANOVA followed by an LSD test ($p < 0.05$), and correlations (PhytOC concentration and Phytolith) were studied using Pearson correlation coefficients with significant levels of $p = 0.05$.

AUTHOR INFORMATION

Corresponding Author

Veeraswamy Davamani − *Department of Environmental Sciences, Tamil Nadu Agricultural University, Coimbatore 641 003 Tamil Nadu, India;* orcid.org/0000-0001-6969-2584; Email: davamani@tnau.ac.in

Authors

Ramasamy Sangeetha Piriya − *Department of Environmental Sciences, Tamil Nadu Agricultural University, Coimbatore 641 003 Tamil Nadu, India*

Srirangarayan Subramanian Rakesh − *Department of Environmental Sciences, Tamil Nadu Agricultural University, Coimbatore 641 003 Tamil Nadu, India*

Ettiyagounder Parameswari − *Department of Environmental Sciences, Tamil Nadu Agricultural University, Coimbatore 641 003 Tamil Nadu, India*

https://doi.org/10.1021/acsomega.1c05592
ACS Omega 2022, 7, 2809−2820

Selvaraj Paul Sebastian − *Agricultural College and Research Institute, Kudumiyanmalai 622104 Tamil Nadu, India*
Periasamy Kalaiselvi − *Horticultural College and Research Institute, Tamil Nadu Agricultural University, Periyakulam 625 604 Tamil Nadu, India*
Muthunalliappan Maheswari − *Department of Environmental Sciences, Tamil Nadu Agricultural University, Coimbatore 641 003 Tamil Nadu, India*
Rangasamy Santhi − *Department of Soil Science and Agricultural Chemistry, Tamil Nadu Agricultural University, Coimbatore 641 003 Tamil Nadu, India*

Complete contact information is available at: https://pubs.acs.org/10.1021/acsomega.1c05592

Notes

The authors declare no competing financial interest.

■ ACKNOWLEDGMENTS

The authors greatly acknowledge the Department of Science and Technology—Science and Engineering Research Board (EMR/2016/005436), New Delhi to accomplish the project work.

■ REFERENCES

(1) Energy Agency, I. *Global Energy Review 2020*; OECD, 2020.
(2) Parr, J. F.; Sullivan, L. A. Comparison of Two Methods for the Isolation of Phytolith Occluded Carbon from Plant Material. *Plant Soil* **2014**, *374*, 45−53.
(3) Yang, J.; Wu, J.; Jiang, P.; Xu, Q.; Zhao, P.; He, S. A Study of Phytolith-Occluded Carbon Stock in Monopodial Bamboo in China. *Sci. Rep.* **2015**, *5*, No. 13292.
(4) Dignac, M. F.; Derrien, D.; Barré, P.; Barot, S.; Cécillon, L.; Chenu, C.; Chevallier, T.; Freschet, G. T.; Garnier, P.; Guenet, B.; Hedde, M.; Klumpp, K.; Lashermes, G.; Maron, P. A.; Nunan, N.; Roumet, C.; Basile-Doelsch, I. Increasing Soil Carbon Storage: Mechanisms, Effects of Agricultural Practices and Proxies. A Review. *Agron. Sustainable Dev.* **2017**, *37*, No. 14.
(5) IPCC. *Climate Change 2014 Mitigation of Climate Change - Working Group III Contribution to the Fifth Assessment of the Intergovernmental Panel on Climate Change*, 2014.
(6) Parr, J.; Sullivan, L.; Chen, B.; Ye, G.; Zheng, W. Carbon Bio-Sequestration within the Phytoliths of Economic Bamboo Species. *Glob. Chang. Biol.* **2010**, *16*, 2661−2667.
(7) Nawaz, M. A.; Zakharenko, A. M.; Zemchenko, I. V.; Haider, M. S.; Ali, M. A.; Imtiaz, M.; Chung, G.; Tsatsakis, A.; Sun, S.; Golokhvast, K. S. Phytolith Formation in Plants: From Soil to Cell. *Plants* **2019**, *8*, 249.
(8) Gao, H.; Zhai, S.; Sun, Z.; Liu, J.; Tong, C. Differences in Biomass and Silica Content in Typical Plant Communities with Ecotones in the Min River Estuary of Southeast China. *PeerJ* **2019**, *7*, No. e7218.
(9) Douze, K.; Lespez, L.; Rasse, M.; Tribolo, C.; Garnier, A.; Lebrun, B.; Mercier, N.; Ndiaye, M.; Chevrier, B.; Huysecom, E. A West African Middle Stone Age Site Dated to the Beginning of MIS 5: Archaeology, Chronology, and Paleoenvironment of the Ravin Blanc I (Eastern Senegal). *J. Hum. Evol.* **2021**, *154*, No. 102952.
(10) Parr, J. F.; Sullivan, L. A. Soil Carbon Sequestration in Phytoliths. *Soil Biol. Biochem.* **2005**, *37*, 117−124.
(11) Alexandre, A.; Balesdent, J.; Cazevieille, P.; Chevassus-Rosset, C.; Signoret, P.; Mazur, J. C.; Harutyunyan, A.; Doelsch, E.; Basile-Doelsch, I.; Miche, H.; Santos, G. M. Direct Uptake of Organically Derived Carbon by Grass Roots and Allocation in Leaves and Phytoliths: 13C Labeling Evidence. *Biogeosciences* **2016**, *13*, 1693−1703.
(12) Alexandre, A.; Basile-Doelsch, I.; Delhaye, T.; Borshneck, D.; Mazur, J. C.; Reyerson, P.; Santos, G. M. New Highlights of Phytolith Structure and Occluded Carbon Location: 3-D X-Ray Microscopy and NanoSIMS Results. *Biogeosciences* **2015**, *12*, 863−873.
(13) Song, Z.; Liu, C.; Müller, K.; Yang, X.; Wu, Y.; Wang, H. Silicon Regulation of Soil Organic Carbon Stabilization and Its Potential to Mitigate Climate Change. *Earth-Sci. Rev.* **2018**, *185*, 463−475.
(14) Yin, J.; Yang, X.; Zheng, Y. Influence of Increasing Combustion Temperature on the AMS 14 C Dating of Modern Crop Phytoliths. *Sci. Rep.* **2014**, *4*, No. 6511.
(15) Huisman, S. N.; Raczka, M. F.; McMichael, C. N. H. Palm Phytoliths of Mid-Elevation Andean Forests. *Front. Ecol. Evol.* **2018**, *6*, No. 193.
(16) Green, S. W. Phytolith Analysis: An Archaeological and Geological Perspective. By Dolores R. Piperno. *Am. J. Archaeol.* **1991**, *95*, 741.
(17) Piperno, D. R. *Phytolyth Analysis: An Archaeological and Geological Perspective*; Elsevier, 2014.
(18) Prychid, C. J.; Rudall, P. J.; Gregory, M. Systematics and Biology of Silica Bodies in Monocotyledons. *Bot. Rev.* **2003**, *69*, 377−440.
(19) Chen, S. T.; Smith, S. Y. Phytolith Variability in Zingiberales: A Tool for the Reconstruction of Past Tropical Vegetation. *Palaeogeogr., Palaeoclimatol., Palaeoecol.* **2013**, *370*, 1−12.
(20) Hodson, M. J. The Development of Phytoliths in Plants and Its Influence on Their Chemistry and Isotopic Composition. Implications for Palaeoecology and Archaeology. *J. Archaeol. Sci.* **2016**, *68*, 62−69.
(21) Buján, E. Elemental Composition of Phytoliths in Modern Plants (Ericaceae). *Quat. Int.* **2013**, *287*, 114−120.
(22) Qi, L.; Li, F. Y.; Huang, Z.; Jiang, P.; Baoyin, T.; Wang, H. Phytolith-Occluded Organic Carbon as a Mechanism for Long-Term Carbon Sequestration in a Typical Steppe: The Predominant Role of Belowground Productivity. *Sci. Total Environ.* **2017**, *577*, 413−417.
(23) Li, Z.; Song, Z.; Li, B. The Production and Accumulation of Phytolith-Occluded Carbon in Baiyangdian Reed Wetland of China. *Appl. Geochem.* **2013**, *37*, 117−124.
(24) Zuo, X. X.; Lü, H. Y. Carbon Sequestration within Millet Phytoliths from Dry-Farming of Crops in China. *Chin. Sci. Bull.* **2011**, *56*, 3451−3456.
(25) Song, Z.; Liu, H.; Si, Y.; Yin, Y. The Production of Phytoliths in China's Grasslands: Implications to the Biogeochemical Sequestration of Atmospheric CO 2. *Glob. Chang. Biol.* **2012**, *18*, 3647−3653.
(26) Parr, J.; Sullivan, L.; Quirk, R. Sugarcane Phytoliths: Encapsulation and Sequestration of a Long-Lived Carbon Fraction. *Sugar Tech* **2009**, *11*, 17−21.
(27) Parr, J. F.; Sullivan, L. A. Phytolith Occluded Carbon and Silica Variability in Wheat Cultivars. *Plant Soil* **2011**, *342*, 165−171.
(28) Chen, C.; Huang, Z.; Jiang, P.; Chen, J.; Wu, J. Belowground Phytolith-Occluded Carbon of Monopodial Bamboo in China: An Overlooked Carbon Stock. *Front. Plant Sci.* **2018**, *9*, No. 1615.
(29) Morcote-Ríos, G.; Bernal, R.; Raz, L. Phytoliths as a Tool for Archaeobotanical, Palaeobotanical and Palaeoecological Studies in Amazonian Palms. *Bot. J. Linn. Soc.* **2016**, *182*, 348−360.
(30) Barroso, F. R. G.; dos Santos Gomes, V.; Carvalho, C. E.; Ledru, M. P.; Favier, C.; Araújo, F. S.; Bremond, L. Phytoliths from Soil Surfaces and Water Reservoirs of the Brazilian Semi-Arid Caatinga. *J. South Am. Earth Sci.* **2021**, *108*, No. 103180.
(31) Qi, L.; Sun, T.; Guo, X.; Guo, Y.; Li, F. Y. Phytolith-Occluded Carbon Sequestration Potential in Three Major Steppe Types along a Precipitation Gradient in Northern China. *Ecol. Evol.* **2021**, *11*, 1446−1456.
(32) Li, Z.; Song, Z.; Parr, J. F.; Wang, H. Occluded C in Rice Phytoliths: Implications to Biogeochemical Carbon Sequestration. *Plant Soil* **2013**, *370*, 615−623.
(33) Li, Z.; Song, Z.; Parr, J. F.; Wang, H. Occluded C in Rice Phytoliths: Implications to Biogeochemical Carbon Sequestration. *Plant Soil* **2013**, *370*, 615−623.
(34) Huang, Z. T.; Jiang, P. K.; Chang, S. X.; Zhang, Y.; Ying, Y. Q. Production of Carbon Occluded in Phytolith Is Season-Dependent in

a Bamboo Forest in Subtropical China. *PLoS One* **2014**, *9*, No. e106843.
(35) Lu, H.; Zhang, J.; Wu, N.; Liu, K. B.; Xu, D.; Li, Q. Phytoliths Analysis for the Discrimination of Foxtail Millet (*Setaria Italica*) and Common Millet (*Panicum Miliaceum*). *PLoS One* **2009**, *4*, No. e4448.
(36) Yang, X.; Song, Z.; Liu, H.; Van Zwieten, L.; Song, A.; Li, Z.; Hao, Q.; Zhang, X.; Wang, H. Phytolith Accumulation in Broadleaf and Conifer Forests of Northern China: Implications for Phytolith Carbon Sequestration. *Geoderma* **2018**, *312*, 36−44.
(37) Song, Z.; Liu, H.; Si, Y.; Yin, Y. The Production of Phytoliths in China's Grasslands: Implications to the Biogeochemical Sequestration of Atmospheric CO 2. *Glob. Chang. Biol.* **2012**, *18*, 3647−3653.
(38) Liu, X.; Li, L.; Bian, R.; Chen, D.; Qu, J.; Wanjiru Kibue, G.; Pan, G.; Zhang, X.; Zheng, J.; Zheng, J. Effect of Biochar Amendment on Soil-Silicon Availability and Rice Uptake. *J. Plant Nutr. Soil Sci.* **2014**, *177*, 91−96.
(39) Jansson, C.; Wullschleger, S. D.; Kalluri, U. C.; Tuskan, G. A. Phytosequestration: Carbon Biosequestration by Plants and the Prospects of Genetic Engineering. *Bioscience* **2010**, *60*, 685−696.
(40) Song, Z.; Liu, H.; Strömberg, C. A. E.; Yang, X.; Zhang, X. Phytolith Carbon Sequestration in Global Terrestrial Biomes. *Sci. Total Environ.* **2017**, *603*−*604*, 502−509.
(41) Song, Z.; Parr, J. F.; Guo, F. Potential of Global Cropland Phytolith Carbon Sink from Optimization of Cropping System and Fertilization. *PLoS One* **2013**, *8*, No. e73747.
(42) Zuo, X. X.; Lu, H. Y.; Gu, Z. Y. Distribution of Soil Phytolith-Occluded Carbon in the Chinese Loess Plateau and Its Implications for Silica-Carbon Cycles. *Plant Soil* **2014**, *374*, 223−232.
(43) Li, Z. M.; Song, Z. L.; Jiang, P. K. Biogeochemical Sequestration of Carbon within Phytoliths of Wetland Plants: A Case Study of Xixi Wetland, China. *Chin. Sci. Bull.* **2013**, *58*, 2480−2487.
(44) Huang, Z.; Li, Y.; Chang, S. X.; Jiang, P.; Meng, C.; Wu, J.; Zhang, Y. Phytolith-Occluded Organic Carbon in Intensively Managed Lei Bamboo (Phyllostachys Praecox) Stands and Implications for Carbon Sequestration. *Can. J. For. Res.* **2015**, *45*, 1019−1025.
(45) Law, K. N.; Daud, W. R. W.; Ghazali, A. Morphological and Chemical Nature of Fiber Strands of Oil Palm Empty-Fruit-Bunch (OPEFB). *BioResources* **2007**, *2*, 351−362.
(46) Bowdery, D. An Enigma Revisited: Identification of Palm Phytoliths Extracted from the 1983 Rapa Nui, Rano Kao2 Core. *Veg. Hist. Archaeobot.* **2015**, *24*, 455−466.
(47) Benvenuto, M. L.; Fernández Honaine, M.; Osterrieth, M. L.; Morel, E. Differentiation of Globular Phytoliths in Arecaceae and Other Monocotyledons: Morphological Description for Paleobotanical Application. *Turk. J. Bot.* **2015**, *39*, 341−353.
(48) Fenwick, R. S. H.; Lentfer, C. J.; Weisler, M. I. Palm Reading: A Pilot Study to Discriminate Phytoliths of Four Arecaceae (Palmae) Taxa. *J. Archaeol. Sci.* **2011**, *38*, 2190−2199.
(49) Mercader, J.; Bennett, T.; Esselmont, C.; Simpson, S.; Walde, D. Phytoliths in Woody Plants from the Miombo Woodlands of Mozambique. *Ann. Bot.* **2009**, *104*, 91−113.
(50) Omar, F. N.; Mohammed, M. A. P.; Baharuddin, A. S. Microstructure Modelling of Silica Bodies from Oil Palm Empty Fruit Bunch (OPEFB) Fibres. *BioResources* **2014**, 938−951.
(51) Batista, W. B.; Rolhauser, A. G.; Biganzoli, F.; Burkart, S. E.; Goveto, L.; Maranta, A.; Pignataro, A. G.; Morandeira, N. S.; Rabadán, M. The Plant Communities of the Savanna of the Palmar National Park (Argentina). *Darwiniana* **2014**, *2*, 5−38.
(52) Lentfer, C. J.; Cotter, M. M.; Boyd, W. E. Particle Settling Times for Gravity Sedimentation and Centrifugation: A Practical Guide for Palynologists. *J. Archaeol. Sci.* **2003**, *30*, 149−168.
(53) Lentfer, C. J.; Green, R. C. Phytoliths and the Evidence for Banana Cultivation at the Lapita Reber-Rakival Site on Watom Island, Papua New Guinea. *Rec. Aust. Museum, Suppl.*; Pacific Odyssey: Archaeology and Anthropology of the Western Pacific. Papers in Honour of Jim Specht, 2004; Vol. *29*, pp 75−88.
(54) Honaine, M. F.; Benvenuto, M. L.; Osterrieth, M. L. An Easy Technique for Silicophytolith Visualization in Plants through Tissue Clearing and Immersion Oil Mounting. *Bol. la Soc. Argentina Bot.* **2019**, *54*, 353−365.
(55) Bokor, B.; Soukup, M.; Vaculík, M.; Vd'ačný, P.; Weidinger, M.; Lichtscheidl, I.; Vávrová, S.; Šoltys, K.; Sonah, H.; Deshmukh, R.; Bélanger, R. R.; White, P. J.; El-Serehy, H. A.; Lux, A. Silicon Uptake and Localisation in Date Palm (Phoenix Dactylifera) − A Unique Association With Sclerenchyma. *Front. Plant Sci.* **2019**, *10*, No. 988.
(56) Rosa, M. F.; Medeiros, E. S.; Malmonge, J. A.; Gregorski, K. S.; Wood, D. F.; Mattoso, L. H. C.; Glenn, G.; Orts, W. J.; Imam, S. H. Cellulose Nanowhiskers from Coconut Husk Fibers: Effect of Preparation Conditions on Their Thermal and Morphological Behavior. *Carbohydr. Polym.* **2010**, *81*, 83−92.
(57) Jonoobi, M.; Khazaeian, A.; Tahir, P. M.; Azry, S. S.; Oksman, K. Characteristics of Cellulose Nanofibers Isolated from Rubberwood and Empty Fruit Bunches of Oil Palm Using Chemo-Mechanical Process. *Cellulose* **2011**, *18*, 1085−1095.
(58) Johar, N.; Ahmad, I.; Dufresne, A. Extraction, Preparation and Characterization of Cellulose Fibres and Nanocrystals from Rice Husk. *Ind. Crops Prod.* **2012**, *37*, 93−99.
(59) Owolabi, A. F.; Haafiz, M. K. M.; Hossain, M. S.; Hussin, M. H.; Fazita, M. R. N. Influence of Alkaline Hydrogen Peroxide Pre-Hydrolysis on the Isolation of Microcrystalline Cellulose from Oil Palm Fronds. *Int. J. Biol. Macromol.* **2017**, *95*, 1228−1234.
(60) Kumneadklang, S.; O-Thong, S.; Larpkiattaworn, S. Characterization of Cellulose Fiber Isolated from Oil Palm Frond Biomass. *Materials Today: Proceedings*; Elsevier, 2019; Vol. *17*, pp 1995−2001.
(61) Chieng, B. W.; Lee, S. H.; Ibrahim, N. A.; Then, Y. Y.; Loo, Y. Y. Isolation and Characterization of Cellulose Nanocrystals from Oil Palm Mesocarp Fiber. *Polymers* **2017**, *9*, No. 355.
(62) Omojola, T.; Lukyanov, D. B.; Cherkasov, N.; Zholobenko, V. L.; Van Veen, A. C. Influence of Precursors on the Induction Period and Transition Regime of Dimethyl Ether Conversion to Hydrocarbons over ZSM-5 Catalysts. *Ind. Eng. Chem. Res.* **2019**, *58*, 16479−16488.
(63) Ahmad, A. L.; Loh, M. M.; Aziz, J. A. Preparation and Characterization of Activated Carbon from Oil Palm Wood and Its Evaluation on Methylene Blue Adsorption. *Dyes Pigm.* **2007**, *75*, 263−272.
(64) Chen, C.; Huang, Z.; Jiang, P.; Chen, J.; Wu, J. Belowground Phytolith-Occluded Carbon of Monopodial Bamboo in China: An Overlooked Carbon Stock. *Front. Plant Sci.* **2018**, *9*, No. 1615.
(65) EPA. Office of Research & Development. *Method 415.3 - Measurement of Total Organic Carbon, Dissolved Organic Carbon and Specific UV Absorbance a 254 nm in Source Water and Drinking Water*, 2015.
(66) Han, N.; Yang, Y.; Gao, Y.; Hao, Z.; Tian, J.; Yang, T.; Song, X. Determining Phytolith-Occluded Organic Carbon Sequestration Using an Upgraded Optimized Extraction Method: Indicating for a Missing Carbon Pool. *Environ. Sci. Pollut. Res.* **2018**, *25*, 24507−24515.
(67) Brunauer, S.; Emmett, P. H.; Teller, E. Adsorption of Gases in Multimolecular Layers. *J. Am. Chem. Soc.* **1938**, *60*, 309−319.

https://doi.org/10.1021/acsomega.1c05592
ACS Omega 2022, 7, 2809−2820